Manufacture of Hot Forging Cables and Arc Additives

Lavpreet Singh, Department of Mechanical Engineering,
Galgotias University, Yamuna Expressway
Greater Noida, Uttar Pradesh
Email ID: punstu@gmail.com

ABSTRACT: In this research a new form of manufacturing of wire and arc additives (WAAM), based on hot forging. The material is forged locally immediately after deposition during WAAM, and viscoelastic deformation occurs at high temperatures in-situ. Recrystallization of the previous solidification structure happens in the subsequent deposition of the sheet, which refines the microstructure. This version was called hot forging wire and arc additive manufacturing (HF-WAAM), due to its resemblance to hot forging. For the development of AISI316L stainless steel samples a customized WAAM torch was produced, manufactured, and tested. Forging forces 17 N and 55 N were applied to bend the material plastically. The results showed that this new variant refines the solidification microstructure and decreases the effects of texture, as determined by experiments with high-energy synchrotron X-ray diffraction, without interrupting the additive production cycle. Mechanical characterisation was accomplished and improvements were made on both yield strength and overall tensile strength. In addition, HF-WAAM has been observed to significantly affect porosity; pores created during the process have been closed by the process of hot forging. Since deformation occurs at high temperatures, the forces involved are minimal, and the WAAM equipment has no unique stiffness requirements, thus allowing this new model to be integrated into traditional moving equipment such as multi-axis robots or 3-axis table used in WAAM.

KEYWORDS: Directed Energy Deposition, Forging, Grain Refining, Wire and Arc Additive Manufacturing, Viscoplastic Deformation, Stainless Steel.

INTRODUCTION

Additive manufacturing techniques have revolutionized the manufacturing industry by producing complex-shaped structures with their ability. There are many additive manufacturing technologies for metals, such as selective laser melting (SLM) and selective laser sintering (SLS), which use added material in powder form, and wire and arc additive manufacturing (WAAM) which use added material only in wire form. The first two technologies are used to produce good surface finishing parts, but production levels are small, while the deposition rate in WAAM is high, at the cost of surface smoothness. This version is more suitable for large-parts development. WAAM is based on multiphase welding and its metallurgy; thus, the microstructure of the components consists of coarse columnar grain structures as a result of the successive thermal re-melting and solidification cycles [1], [2]. Aside from a large grain size, the mechanical resistance is weak and anisotropic due to which the device can fail prematurely under multi-axial tensile or cyclical demands.

Another potentially negative feature is pore formation. In this case, the presence of pores in parts to be used in structural applications can be important as it is possible to find a substantial decrease in the mechanical properties of the parts depending on their volume fraction and location. It is also a significant problem for non-destructive testing (NDT) and does not guarantee these defects are found.

A critical step towards industrializing Additive Manufacturing is the implementation of non-destructive testing (NDT), which has faced many challenges due to the complex geometry and high surface roughness of the additively produced parts. The potential of computed tomography (CT) and ultrasonic testing has been demonstrated by recent developments in this topic [3]. CT may be costly, however, and poses some limitations with respect to in situ application of NDT. Ultrasonic (UT) methods, in particular, phased ultrasonic array testing, proved to be a feasible technique for inspecting AM parts with high reliability and sensitivity. Nonetheless, this technique requires a plane surface, which is usually done by machining, to ensure proper coupling for the probe. The top surface of the sample is flat with the presented version, which enables the coupling of the ultrasonic and eddy currents probes without the need for post-processing [4]. The presence of both large grain structures and pores has inspired researchers to find methods to reduce these microstructural features, or even remove them. One way of simultaneously raising grain size and porosity is by adding pressure between the deposited layers. Colegrove et al. first applied cold rolling at

interpass after each layer was deposited. A load between 50 and 75kN was needed to achieve successful grain refinement because rolling was applied only when the material was nearly at room temperature (such as 50 ° C) and cold plastic deformation was intended to produce a hardening effect on the material. Once the subsequent layer was deposited the heat transferred to the recrystallization of the grain structure caused by the previously deformed material.

Although this method is efficient in reducing the grain size and collapsing pores that may occur within the deposited sheet, it is time-consuming to wait for the material to cool down before rolling. Zang et al. produced a hot micro-rolling method that follows the movement of the welding torch and forges the welding bead by layer above 800 ° C. Yang et al. produced a hot-rolling method consisting of three rollers that were able to deform the three sides of any deposited material simultaneously with an applied rolling force of 3kN. Both studies revealed improvements in the dimensional precision and mechanical properties of the components generated. These methods however require the manufacture of a completely different additive manufacturing equipment with high structural rigidity. This avoids the use of a commonplace welding source and a robot or XYZ table, and raises process costs, thereby making it less efficient [5].

There has also been analysis of the application of surface treatments such as laser shock peening and ultrasonic peening. Such therapies have shown residual stress reduction and microstructure refinement. However, these processes are less effective compared with the rolling methods to increase the part's geometrical accuracy. In this research a new variant of WAAM to achieve a similar effect while minimizing down times between deposition of layers and the load needed to deform the material: it involves performing a local viscoplastic deformation of the already deposited layers immediately after depositing the material. This will resemble a semi-solid forging process [6]. Dynamic recrystallization of the material may be caused by deforming the as-deposited layer at high temperature and facilitating the collapse of pores that may have formed during the deposition. These two characteristics can be accomplished under a fraction of the load needed when the deformation occurs at low temperatures, i.e., near room temperature.

The presence of recrystallized grains in parts of WAAM has some clear advantages: First, the mechanical strength may increase following the Hall – Petch relationship; then, the presence of refined grains at the top of the deposited layer provides a higher nucleation site density, thus growing the susceptibility to broad grain growth as seen in WAAM deposits. This is especially important for alloys with no transformations in solid state, which are more susceptible to large grain growth during successive thermal cycles [7]. The possible advantage of deforming the as-deposited layers at high temperatures is to enhance waviness and roughness of the surface, thus increasing component precision and reducing material waste in subsequent processes.

A novel variant of WAAM designated as hot forging wire and arc additive manufacture (HF-WAAM) is presented in this report [8]. The principles of the process and its impact on a complete austenitic stainless steel part's microstructure are discussed and debated. A new method is intended to be used to improve the microstructure and mechanical properties of the deposited material. Therefore, as there is no need to wait for the material to cool down to near room temperature this variant can be applied without an increase in development time, which is known to occur while applying cold rolling variant.

PROCESS FUNDAMENTALS

Most of the researchers currently working on WAAM using traditional welding torches that are connected to a moving unit, which is normally a 6-axis robot arm. Conventional welding torches were designed for use by an operator; due to ergonomic and safety considerations, the strength, shielding gas, and wire are fed via the same torch. Those torches are impractical for a WAAM application under these architecture constraints. Research therefore suggest an revolutionary idea of a multi-feed system in which the various inputs can be decoupled and regulated independently, including electrical power, shielding gas, material feed, and a new input consisting of mechanical work / local viscoplastic deformation (Figure 1a).

Overall, HF-WAAM requires the use of a hammer inside the gas nozzle, which a vibrating actuator triggers (Figure 1b). The vibrating actuator can be electromagnetic (solenoid) or mechanical (pneumatic cylinder), and at various frequencies it can operate. The hammer moves with the torch and is triggered while the

material is still being deposited; the element is forged at temperatures close to 900 ° C exceeding the recrystallization temperature for this material (almost 450 ° C); this is similar to a hot forging process and deformation and solidification occurs. HF-WAAM's main aim is to use high-temperature viscoplastic deformation activity to minimize residual stress, improve ductility, remove post-heat treatment operations, and homogenize grain structure. This revolutionary technology reduces the load forging, the tooling and the rigidity of the machinery [9].

Some specific electrical precautions must be taken into consideration. As in gas metal arc welding torches (GMAW), the welding nozzle is electrically isolated from both the main conductor (+) and the component (−). In addition, the vibrating hammer is related electrically to the main conductor (+) by means of a high electrical resistance (R) (Figure 1c). Therefore, if the hammer is raised but stays very close to the WAAM component, the electrical potential of the hammer is the same as that of the main conductor (+), therefore preventing arc ignition. Moreover, the high electrical resistance (R) also prevents the current flow from the part to the hammer when a short circuit is formed since the hammer contacts the part.

Other hammer geometries or part assemblies that can be considered for HF-WAAM include: I a hammer with a circular wire-concentric crown geometry, ii) a hammer outside the gas nozzle and iii) the gas nozzle itself as a hammer. The last two allow the HF-WAAM to be applied in nonlinear deposition paths as the forged region can completely rotate 360 ° and apply this variant to the manufacturing of multi beads [10].
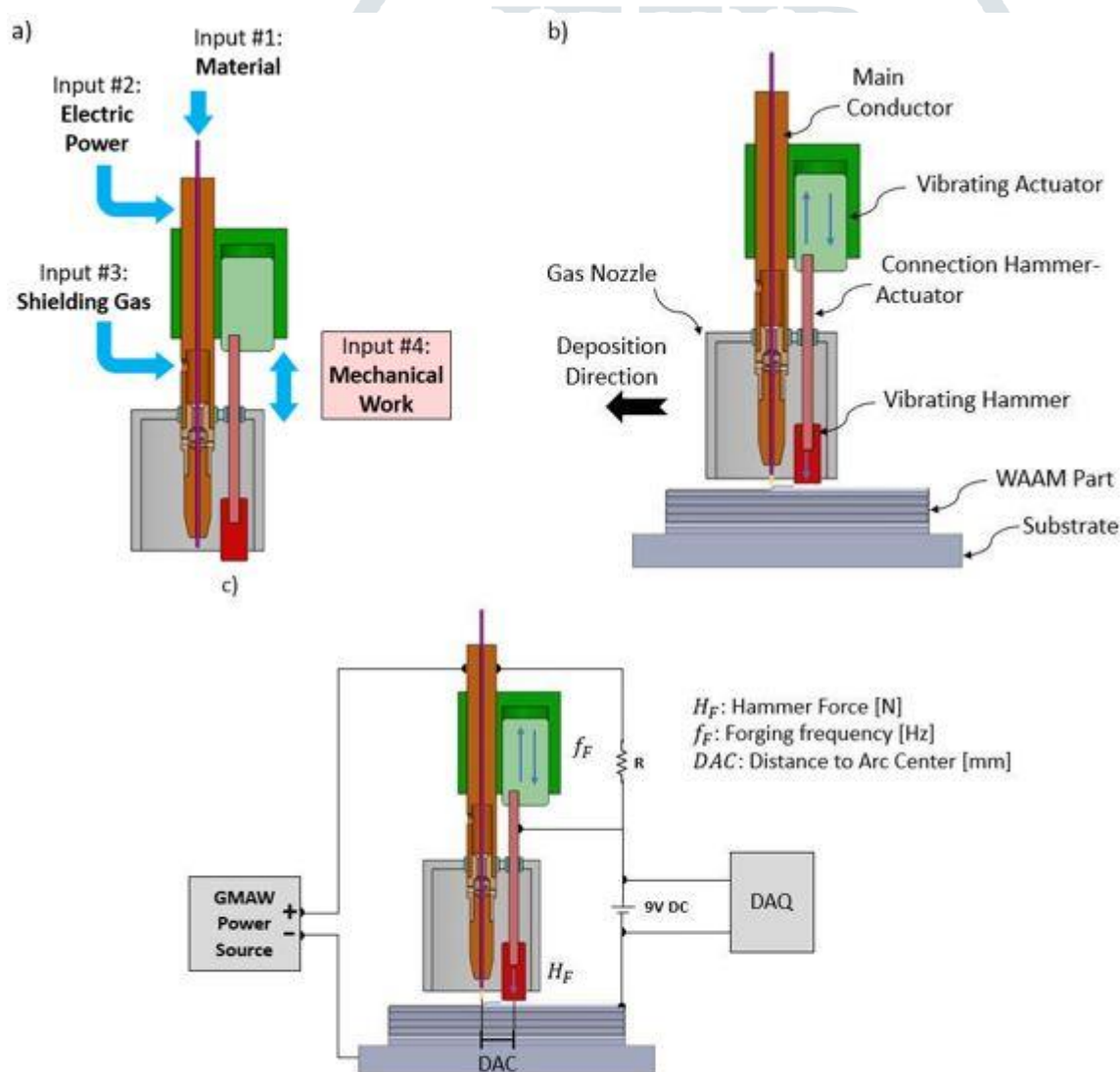

Figure 1 – Schematic Representation of a) HF-WAAM Inputs, b) HF-WAAM Components, and c) Process Parameters and Electrical Scheme Used To Avoid Arc between the Vibrating Hammer and Welding Torch

In addition, the hammer may be designed to reduce the waviness of the component and increase geometric precision. WAAM adds an additional set of process parameters (Figure 1c) which may affect the end

metallurgical, mechanical, and geometric properties of the component [11]. This package contains the following parameters: force forging, F[N]; frequency forging, f_F[Hz]; distance to the middle of the arc, DAC[mm]; geometry for the hammer. The area forged in each cycle depends on the hammer's lower surface geometry and the forging step, Fs [mm] that is the distance the hammer travelled in one cycle; this is a function of f_F and travel speed, $V_{deposition}$ [m / s]. Thus the following equation gives the forging step:

$$F_s = \frac{1}{f_F} \times V_{deposition}$$

The forging step must be lower than the hammer radius for a cylindrical hammer, in order to avoid leaving unforged areas between steps. To assess the pressure applied, the region forged over each cycle must be established. The area forged is shown in Figure 2 for this particular geometry, and can be calculated by equations.
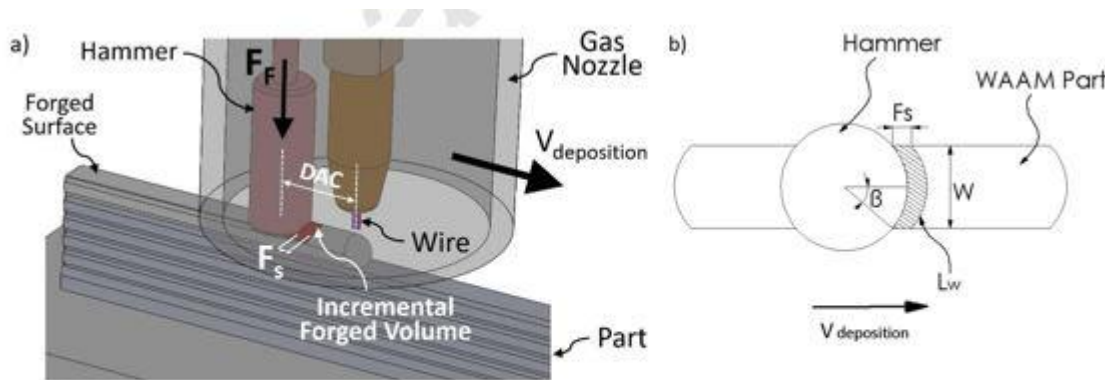

Figure 2 – Schematic Representation of the Forged Area at Each Step: a) Isometric View (3D); b) Top View (2D)

$$A = F_s \times l_w$$

$$l_w = \frac{2\pi R_m \times 2\beta}{360}$$

$$\beta = \sin^{-1}\left(\frac{W}{2R_m}\right)$$

Where: Rm[mm] is the hammer radius, lw [mm] the arc length, W [mm] the bead width, and

β [°] the angle of the arc half-length.

MATERIALS AND METHODS

A custom WAAM torch (Figure 3) has been connected to a moving head inside a working envelope of 2760 / 1960 / 2000 mm3. A KEMPY PRO MIG 3200 power source was used to deposit a stainless steel 1 mm diameter AISI316L on a mild steel substrate. For vibrating actuators, two pneumatic cylinders were used: a FESTO ADVC-6-5-A-P with a produced force of 17 N at 0.6 MPa, and an SMCCU10-10 T with a produced force of 55 N at 0.6 MPa. An M6 leadscrew attached both the pneumatic cylinders to the steel tool hammer. The pneumatic cylinders were actuated using a 5/2-way bi-stable Festo VUVS-LK20 solenoid valve operated by a Data Acquisition (DAQ) system.

The length of the samples produced was set at 100 mm, and the interval of time between depositions was set at 2 min. A one-way method for deposition was introduced, in which the torch always returned to the same starting point. To test the effect of HF-WAAM, four samples were produced: one as-built sample, and three samples with 17, 55 N forging powers. The first two hot-forged samples were produced using a 10

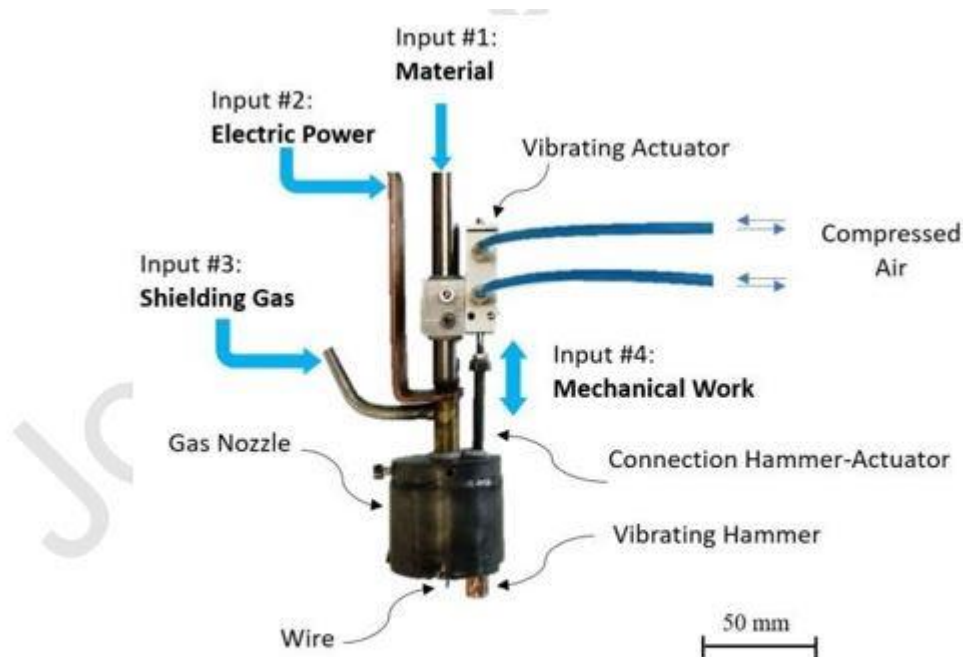mm diameter cylindrical hammer and the last one was produced using a 3 x 9 mm2 contact area parallelepiped hammer.

Figure 3 – Customized Hot Forging Wire and Arc Additive Manufacturing (HF-WAAM) Multi-Feed Device

To prove its efficacy in reducing the amount of pores, they repeated the same samples without shielding air [12]. Table 1 displays the process parameters that were used to deposit and deform the material. It should be remembered that a pneumatic actuator prescribes the hammer force and, thus, the force applied remains constant throughout the component as the compressed air remains at constant pressure throughout the entire process.

Table 1 –Process Parameters Used During HF-WAAM.

Welding mode	Gas metal arc welding – continuous mode (DC+)
Number of layers	10
Forging frequency	10 Hz
Distance to arc center	14 mm
Wire feed speed	4 m/min
Travel speed	360 mm/min
Voltage	20 V DC
Contact tip to work distance	6 mm
Shielding gas	Argon 99.99 %
Gas flow rate	12 l/min

To determine the intermittent contact between the hammer and the part, an electric circuit was set up. The circuit uses a 9 V battery to create a current loop and when it comes into contact with the component, the hammer acts as a switch (Figure 1 c). The contact period (short circuit / low voltage) and the non-contact duration (open circuit / high voltage) can therefore be defined by using a DAQ system to calculate the voltage of the batteries. Figure 4 displays the hammering effect over a time interval of 1s; it supports a hammering frequency of 10 Hz and a service cycle of approximately 48 per cent.
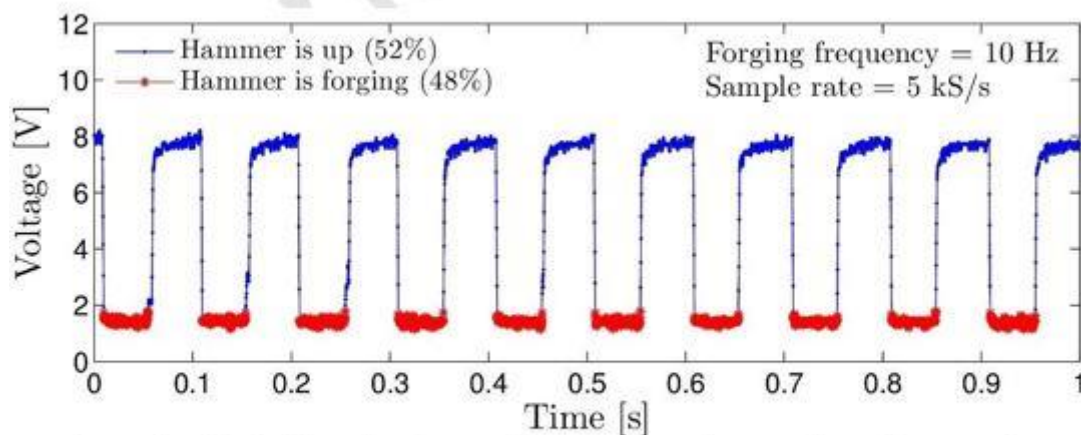
Figure 4 – Variation of voltage with respect to time to detect hammering during deposition

A thermographic infrared camera Fluke TI400 was used during fabrication to monitor the temperature of the components. The camera had a precision of ±2 percent, a maximum of 1200 ° C, a refresh rate of 9 Hz, and a resolution of 320 around 240 pixels. It checked the emissivity of 0.7 using thermocouples. During preparation the temperature was measured at every point using the SmartView acquisition app. Cross-sections were cut, polished, and engraved with Vilella's reagent from the centre of each sample. The metallographic study was conducted using an inverted optical microscope of Leica DMI 5000 M. The geometrical properties of the parts were determined using the Adobe Photoshop CS6 image program. X-ray diffraction was conducted at Petra III / DESY's beamline P07 High Energy Materials Science (HEMS) using a wavelength of 0.1426 Å (87.1keV) and a 1 mm incident beam. A Perkin- Elmer detector was mounted at 1.40 m from the sample, with a pixel size of 200 x 200μm. Calibration was performed using LaB6 powder. The raw 2D images from Debbye-Scherrer provide qualitative details on the grain size and texture of the content analysed [13].

Uniaxial tensile tests were conducted on an AG500Kng Autograph Shimadzu system model fitted with an SFL-50kN AG Shimadzu load cell with a total capacity of 50kN. A crosshead displacement speed of 0.01 mm / s was placed, and the experiments at room temperature were carried out. Specimens were collected from the As-built and 55 N hammered samples in the vertical direction for uniaxial tensile testing. For each condition three specimens were tested to determine the reproducibility of the mechanical properties of the pieces. A TM3030 plus Voltage Table top Scanning Electron Microscope (SEM) analysed the fracture surfaces of both as-built and hot-forged samples at an acceleration voltage of 15keV.

RESULTS AND DISCUSSION

Figure 5 shows the samples that are produced with specific forging forces, hammer geometries and gas flow rate shielding. By using shielding gas to facilitate the creation of pores, the experiments were deliberately repeated and thus characterize the feasibility of the hot forging variant in collapsing and the porosity in the parts generated. The height variations for the one-way deposition technique at the beginning and end of the deposition arise because of the rapid cooling and the small amount of heat accumulated at the beginning of the deposited sheet, as compared to the large amount of heat accumulated at the end of each deposited sheet. This allows the program to correct the processing parameters. It is evident that the hammer has a

considerable impact on the geometry of the bead as it flattens the layers along its duration, thus diminishing this feature which requires parametric correction inline.
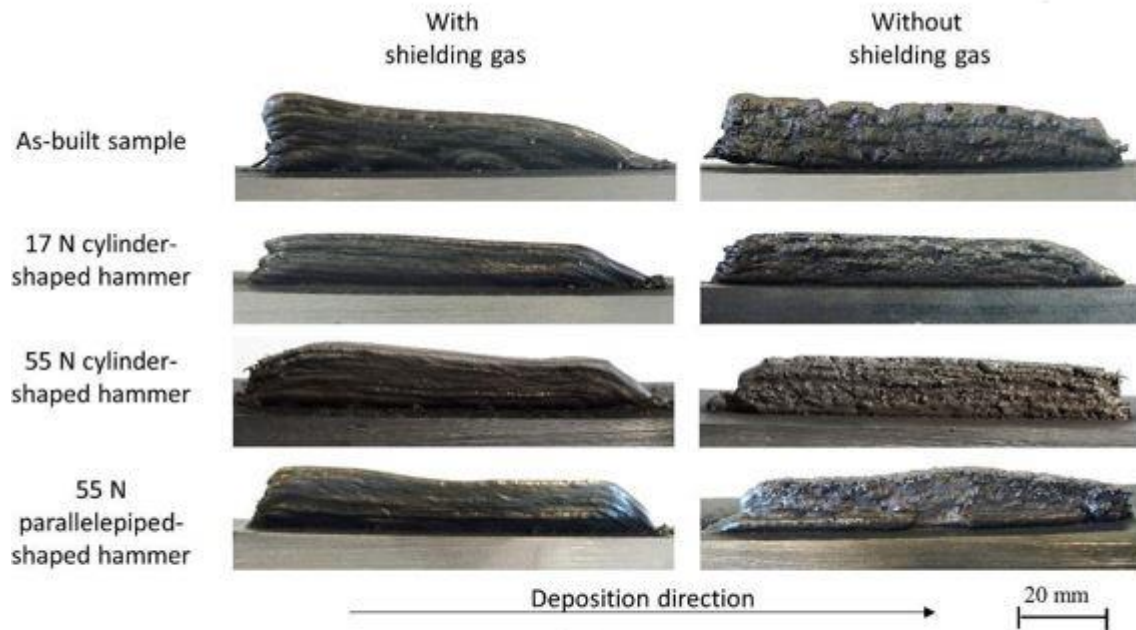

Figure 5 – Overall Aspect of the Samples Produced With Different Process Parameters

Owing to the constant process conditions under which hammering is performed, the flat top surfaces in this version are achieved. Since deformation often happens at the same distance of the electric arc, the temperature of the material will be the same, and hence its properties. This means it will result in even flat surface as shown by keeping the force constant during the cycle. In addition, the forging step in the deposition was 0.6 mm, meaning the hammer advances 0.6 mm at each stroke. The remaining length (9.4 mm) serves as a limiter as the hammer has a diameter of 10 mm, facilitating a consistent height in the course of the deposition.
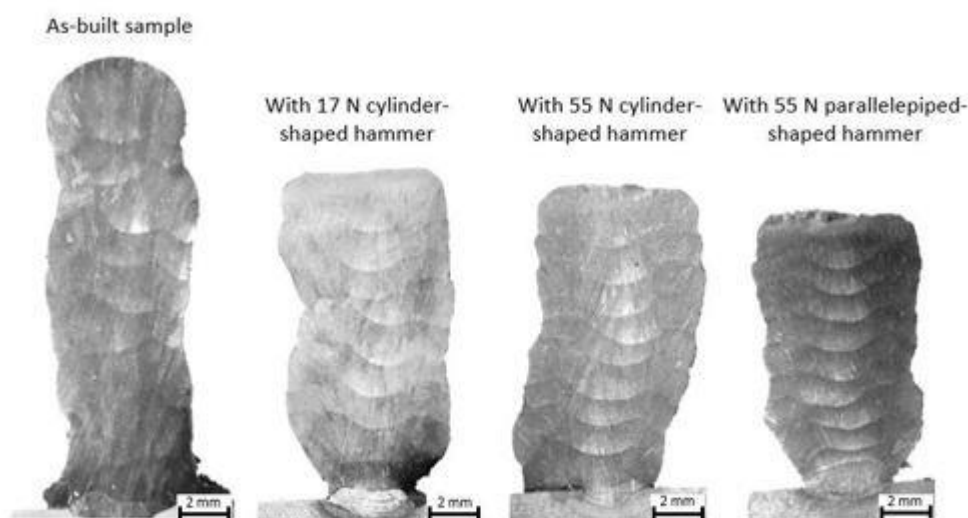

Figure 6 – Cross-Section of the Samples Produced With Shielding Gas

Hot forging effects are noticeable in the cross-section macrographs extracted from each sample that is produced with shielding gas (Figure 6). With hot forging, as the forging forces increased the layers became larger and thinner, and this is particularly evident for the sample produced with the rectangular hammer. That is demonstrated by the decreased rectangular hammer contact area (27 mm2) relative to the circular-shaped one (78.5 mm2). The tension increases by raising the contact zone; therefore, the deformation

increases. Another observation is the flattening effect of the last deposited layer which assists in the subsequent layer deposition.

They measured the width and height of each part. Figure 7 shows respective mean and standard deviation values. The measurements of the element are contrasted with the control specimen. The height of the parts decreases as the forging force increases, and the width increases due to volume conservation in the field of plastic deformation.
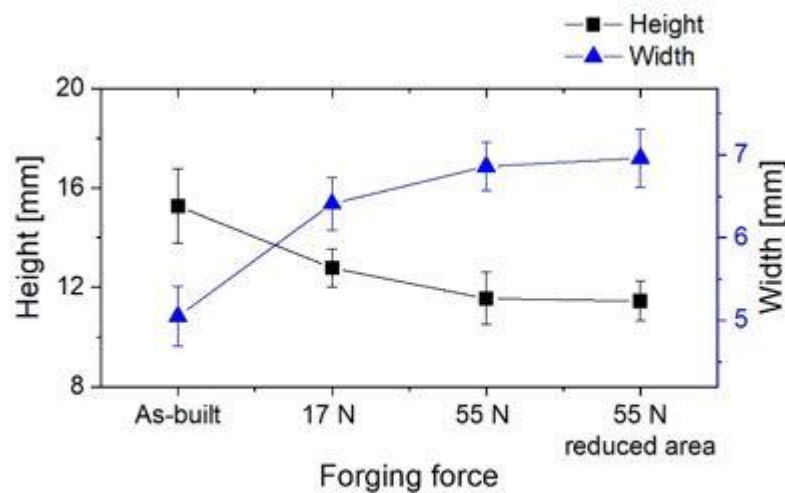

Figure 7 – Height and Width Measurements of Each Produced Sample

In this work the feasibility of the latest HF-WAAM model is demonstrated in promoting grain refinement and pore collapse. It is predicted, but must be verified in future research if this novel WAAM variant has an effect on the microstructure in the deposited materials and also its influence on the fatigue behaviour of the structural parts generated by HF-WAAM.

CONCLUSION

This paper introduces a new variant of WAAM, and the physical and metallurgical concepts on which it is based; this variant is called HF-WAAM and is based on hot forging between deposited layers. A WAAM torch has been developed, manufactured and tested to match your needs. This version demonstrated promise for industrial applications, with the following advantages:-Equipment used. Since the deformation occurs at high temperatures, there are small forces involved, and the rigidity of the hot forging equipment is lower than that of the cold rolling variant. The hot forging version can also be integrated into traditional moving equipment used in WAAM, such as XYZ table or robot with 6 axes. Since the forces are low, the energy expended is nearly zero, which is a valuable added benefit. The hot forging effect refines the microstructure of the solidification while enhancing the mechanical strength. The yield strength increased from 360 to 450 MPa relative to the construction component, the ultimate tensile strength increased from 574 to 622, while the fracture elongation decreased from 32 to 28 percent. In addition, existing internal pores collapse under the forging force which is beneficial to the in-service actions of manufactured additive components.

REFERENCES

[1] J. Sui *et al.*, "Texturation boosts the thermoelectric performance of BiCuSeO oxyselenides," *Energy Environ. Sci.*, 2013.

[2] Z. Gronostajski, M. Kaszuba, S. Polak, M. Zwierzchowski, A. Niechajowicz, and M. Hawryluk, "The failure mechanisms of hot forging dies," *Mater. Sci. Eng. A*, 2016.

[3] P. Rodrigues *et al.*, "Microstructural characterization of NiTi shape memory alloy produced by rotary hot forging," *Powder Diffr.*, 2017.

[4] J. Málek, F. Hnilica, J. Veselý, and B. Smola, "Heat treatment and mechanical properties of powder metallurgy processed Ti-35.5Nb-5.7Ta beta-titanium alloy," *Mater. Charact.*, 2013.

[5] A. Foydl *et al.*, "Manufacturing of steel-reinforced aluminum products by combining hot extrusion and closed-die forging," in *Key Engineering Materials*, 2012.

[6] M. Li, J. Li, X. Bao, X. Mu, and X. Gao, "Magnetostrictive Fe82Ga13.5Al4.5 wires with large Wiedemann twist over wide temperature range," *Mater. Des.*, 2017.

[7] S. K. Chaurasia, U. Prakash, K. Chandra, and P. S. Misra, "Comparisons of sintered technology with powder forging for Fe-P soft magnetic alloys," in *Materials Science Forum*, 2012.

[8] C. Dahnke, F. Kolpak, T. Kloppenborg, and A. E. Tekkaya, "Manufacturing of reinforced profiles by means of combined continuous and discontinuous composite extrusion," in *Materials Today: Proceedings*, 2019.

[9] I. Pfeiffer *et al.*, "Compound forging of hot-extruded steel-reinforced aluminum parts," *Steel Res. Int.*, 2012.

[10] L. Ma, J. Xia, and J. R. Dahn, "Ternary Electrolyte Additive Mixtures for Li-Ion Cells that Promote Long Lifetime and Less Reactivity with Charged Electrodes at Elevated Temperatures," *J. Electrochem. Soc.*, 2015.

[11] G.-Y. Kim and J. R. Dahn, " ARC Studies of the Effects of Electrolyte Additives on the Reactivity of Delithiated Li 1-x [Ni 1/3 Mn 1/3 Co 1/3]O 2 and Li 1-x [Ni 0.8 Co 0.15 Al 0.05]O 2 Positive Electrode Materials with Electrolyte ," *J. Electrochem. Soc.*, 2014.

[12] J. Geder, H. E. Hoster, A. Jossen, J. Garche, and D. Y. W. Yu, "Impact of active material surface area on thermal stability of LiCoO 2 cathode," *J. Power Sources*, 2014.

[13] M. Sol-Sánchez, J. Castro, C. G. Ureña, and J. M. Azañón, "Stabilisation of clayey and marly soils using industrial wastes: pH and laser granulometry indicators," *Eng. Geol.*, 2016.